Acta Crystallographica Section C
Crystal Structure Communications
ISSN 0108-2701

Infinite ladder-like chains organized into a three-dimensional zigzag supramolecular architecture in 9-deazahypoxanthine

Radka Novotná and Zdeněk Trávníček*

Regional Centre of Advanced Technologies and Materials, Department of Inorganic Chemistry, Faculty of Science, Palacký University, 17. listopadu 12, CZ-771 46 Olomouc, Czech Republic
Correspondence e-mail: zdenek.travnicek@upol.cz

Received 12 December 2012
Accepted 13 December 2012
Online 5 January 2013

The asymmetric unit of the title compound, $C_6H_5N_3O$, consists of discrete molecules of 9-deazahypoxanthine [systematic name: 3*H*-pyrrolo[3,2-*d*]pyrimidin-4(5*H*)-one]. The structure displays N—H···O hydrogen bonding, connecting the molecules into centrosymmetric dimers. These dimers are then connected by N—H···N hydrogen bonds into a ladder-like chain along the *c* axis. The secondary structure is stabilized by weak noncovalent contacts of the C—H···O and C—H···C types, as well as by π–π stacking interactions, which organize the structure into a zigzag architecture.

Comment

3,5-Dihydropyrrolo[3,2-*d*]pyrimidines, and in particular the title compound, 9-deazahypoxanthine, (I), have become of great interest because of the potential pharmaceutical use of their derivatives (Montgomery *et al.*, 1993; Bzowska *et al.*, 2000). C9-Substituted 9-deazahypoxanthines (immucillins) are powerful inhibitors of purine nucleoside phosphorylase (PNP), which reversibly catalyses the cleavage of purine nucleosides to the corresponding free bases. The activity of this enzyme is most probably required for normal human T-cell proliferation, and therefore PNP inhibitors represent a novel class of potential selective immunosuppressive agents and may be useful for the treatment of autoimmune disorders, such as psoriasis and rheumatoid arthritis, and other T-cell proliferative disorders, such as organ-transplant rejection and adult T-cell leukaemia (Bantia *et al.*, 2001). Moreover, two members of the immucillin family, *viz.* immucillin-H [BCX-1777, 1-(9-deazahypoxanthin)-1,4-dideoxy-1,4-imino-D-ribitol)] and DADMe-immucillin-H (BCX-4208, 7-{[(3*R*,4*R*)-3-hydroxy-4-(hydroxymethyl)pyrrolidin-1-yl]methyl}-1,5-dihydropyrrolo[3,2-*d*]pyrimidin-4-one), are currently in human clinical trials for the treatment of T- and B-cell cancers and autoimmune diseases (Clinch *et al.*, 2009). Research on 9-deazahypoxanthine derivatives has been incessant and more derivatives have been prepared and tested as antiproliferative (Otmar *et al.*, 2004) or antidiabetic (Sutton *et al.*, 2012) agents.

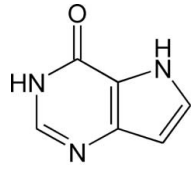

(I)

Even though (I) has long been known and is well characterized, a search of the Cambridge Structural Database (Version 5.33, August 2012 update; Allen, 2002) gave 17 structures involving the 9-deazahypoxanthine group and none of these showed the structural arrangement of the unsubstituted title molecule. All the data deposited so far describe the structures of variously mono-, bi- and trisubstituted 9-deazahypoxanthine derivatives exhibiting different biological properties. For many of these derivatives, (I) served as a synthetic precursor. For example, 6-chloro-9-deazapurine is easily available from 9-deazahypoxanthine, and it may then serve as a perfect precursor for the preparation of 9-deaza-analogues of C6-substituted purines, such as the potent cyclin-dependent kinase inhibitor olomoucine (Čapek *et al.*, 2003). It is well established that knowledge of the molecular structure and crystal packing of a compound provides the necessary information for defining possible structure–property relationships, involving different polymorphs with varying physical and chemical properties important in pharmacology, or for the identification of possible coordination sites when the compound acts as a ligand in a metal complex. Therefore, in connection with the medicinal potential of 9-deazahypoxanthine derivatives, the constant search for more potent analogues and their potential use as ligands in the preparations of biologically active transition metal complexes, the effort to provide a thorough structural description arising from X-ray structure determination accompanied by a combination of analytical methods such as multinuclear NMR spectroscopy or mass spectrometry is unambiguously justified. In this work, we report not only the detailed structural determination of 9-deazahypoxanthine, (I), in the solid state by single-crystal X-ray analysis, but also a thorough characterization of this compound by a wide spectrum of other methods.

Before the isolated title compound was subjected to crystallization attempts, it was fully characterized after preparation in order to confirm its identity and chemical purity. The techniques used for the study of the composition of (I) involved elemental analysis and spectroscopic (IR, MS and NMR) methods. The NMR spectroscopic measurements unambiguously confirmed the composition of (I). It should be pointed out that full interpretations of the ^{1}H, ^{13}C and ^{15}N NMR spectra of (I) have not been reported in the literature thus far.

The molecular structure of (I) consists of discrete molecules of 9-deazahypoxanthine (Fig. 1). The molecule contains nearly coplanar pyrimidine and pyrrole rings [dihedral angle =

  doi:10.1107/S0108270112050767

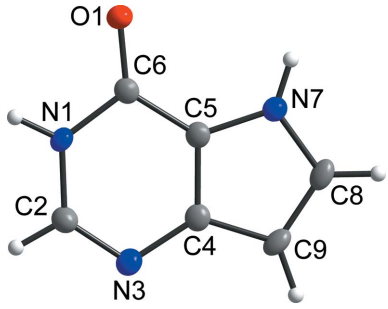

Figure 1
The molecular structure of (I), showing the atom-numbering scheme. Displacement ellipsoids are drawn at the 50% probability level.

0.70 (7)°]. Both rings, *i.e.* pyrimidine as well as pyrrole, deviate from planarity (Nardelli, 1995), the maximum deviations from the mean planes being 0.004 (2) and 0.005 (2) Å for atom C4 in the case of the pyrimidine and pyrrole rings, respectively. While the molecule is essentially planar, with the maximum deviation being 0.014 (2) Å for atom C9, statistically, it deviates from planarity significantly (Nardelli, 1995).

The molecule of (I) can formally be derived from the hypoxanthine skeleton by substituting atom N9 for a C atom. Two polymorphs of hypoxanthine have been published so far, *viz*. the triclinic form (Schmalle *et al.*, 1988) and the monoclinic form (Yang & Xie, 2007). Comparing the structural parameters and focusing on bond angles, the most significant differences would be expected in the vicinity of the substituted C9/N9 atoms, as well as at the N7 site, more specifically in the case of the C5—N7—C8 and C4—C9—C8 angles in (I), and the C5—N7—C8 and C4—N9—C8 angles in hypoxanthine. The expected changes can be explained not only on the basis of the presence of different atoms in the 9-position, but also in connection with the protonation at atom N7 in (I), in contrast with hypoxanthine, where the N9 site is primarily protonated. While the differences in the angles at N7 are conclusively significant, the substitution of N9 in hypoxanthine by C9 in (I) does not bring about a significant difference in the angle at position 9. On the other hand, the bond angles in (I) are comparable with those reported for a monosubstituted derivative of (I), namely 9-deazainosine monohydrate [9-(2-hydroxyethoxymethyl)-9-deazahypoxanthine monohydrate; Otter *et al.*, 1992]. For a comparison of selected bond angles, see Table 1.

The crystal structure consists of the molecules of (I) organized into one-dimensional ladder-like chains along the *c* axis (Fig. 2) by hydrogen bonding of moderate strength. Two heteroaromatic amine groups are involved in the formation of two main supramolecular ring synthons (Bernstein *et al.*, 1995): (*a*) a centrosymmetric amide-like $R_2^2(8)$ ring involving the donor N1—H group and atom O1 as an acceptor and (*b*) an asymmetric $R_2^2(8)$ ring involving N7—H and C2—H donors, and atoms O1 and N3 as acceptors, respectively. These hydrogen bonds provided by the heteroaromatic amine groups are of different strengths, as can be seen from the donor–acceptor distances (Table 2). This difference in donor–acceptor distance can be rationalized on the basis of the different types of hydrogen-bond acceptors, where the lower electronegativity of nitrogen with respect to oxygen determines the different qualities of the noncovalent contacts. The C2—H2···O1^{iii} contact is rather long in comparison with the aforementioned hydrogen bonds (Table 2), but its distance classifies it in the group of very short C—H···O hydrogen bonds (Desiraju & Steiner, 2001).

The individual one-dimensional ladder-like chains are interconnected by π–π stacking interactions, thus forming a

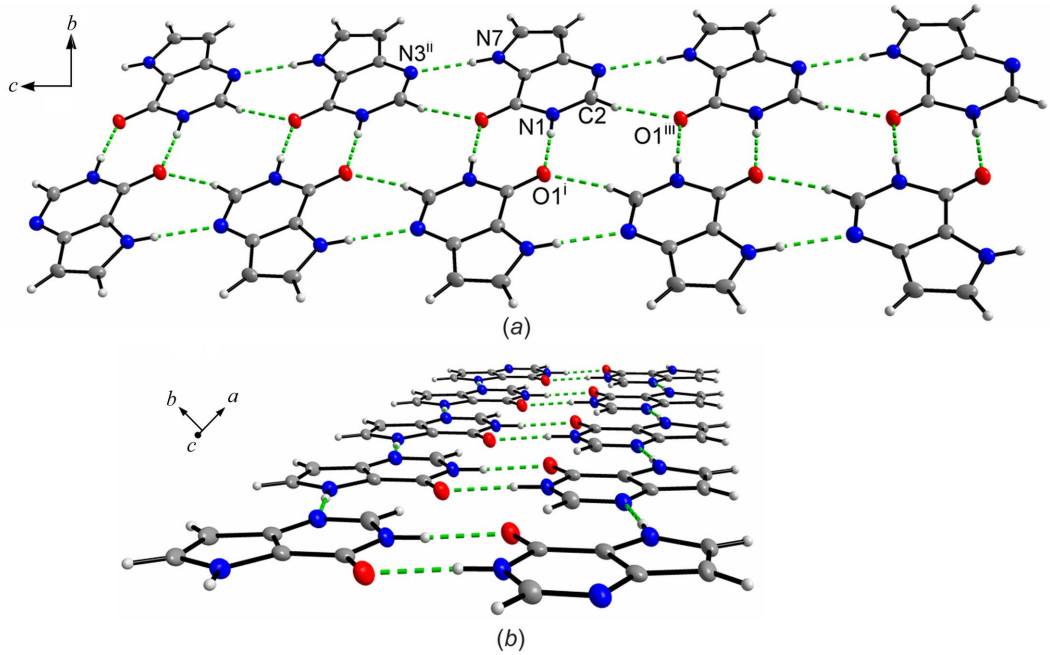

Figure 2
(*a*) A view of (I) along the *a* axis, showing the N—H···O, N—H···N and C—H···O hydrogen bonding (dashed lines). (*b*) A view of the one-dimensional ladder-like chain along the *c* axis, showing its planarity. [Symmetry codes: (i) $-x+2, -y, -z+1$; (ii) $x, y, z+1$; (iii) $x, y, z-1$.]

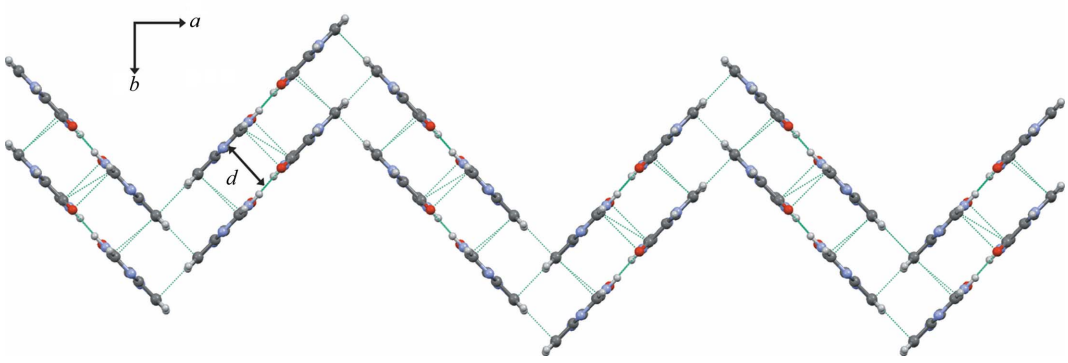

Figure 3
Part of the crystal structure of (I), showing the formation of layers of ladder-like chains stacked by π–π interactions, with a distance d between neighbouring layers of 3.193 Å, and the formation of the zigzag supramolecular architecture along the c axis. Dotted lines indicate intermolecular interactions.

two-dimensional arrangement. The distance between the planes fitted through the non-H atoms of ten molecules in each plane forming the one-dimensional chain is d = 3.193 Å (Fig. 3). The closest C···C contact is between atoms C9 and C2^{iv} [C···C = 3.267 (3) Å; symmetry code: (iv) $x-1, y, z$]. The distance between these best-fit planes is significantly shorter than that between the individual aromatic rings, which are thus not placed directly above one another, as demonstrated by the centroid–centroid distance [$Cg1\cdots Cg1^{iv}$ = 4.8315 (12) Å, where $Cg1$ is the centroid of the non-H atoms of (I)]. In other words, neighbouring layers are shifted by 3.626 Å.

Additional weak noncovalent contacts are also present within the crystal structure of (I), *viz.* C9—H9···C8^{v} [C···C = 3.557 (3) Å; symmetry code: (v) $x-\frac{1}{2}, -y+\frac{1}{2}, z-\frac{1}{2}$]. This connects the individual infinite ladder-like chains, which results in the organization of the crystal structure into a three-dimensional zigzag architecture, as viewed along the c axis (Fig. 3). The least-squares planes of the molecules in the one-dimensional ladder-like chains organized into the zigzag structure are nearly perpendicular; the dihedral angle is about 86°.

Experimental

The title compound, (I), was prepared by a modification of the three-step procedure of Kamath *et al.* (2009) and was characterized as a chemical individuum. The modifications to the published synthesis lie primarily in a shortening of the reaction time and differences in the purification methods for obtaining the intermediates in the reaction process. The first step, as a result of the applied modifications, was complete after *ca* 4 h, in contrast with the published procedure with a reaction completion time of 24 h. Diethylaminomalonate hydrochloride (0.05 mol), ethyl (ethoxymethylene)cyanoacetate (0.05 mol) and sodium methoxide (0.152 mol) in methanol (125 ml) were mixed carefully at a temperature below ambient conditions (in an ice bath). The reaction solution was then treated with ultrasound for *ca* 15 min before being refluxed for 4 h. The light-yellow solid product of dimethyl amino-1*H*-pyrrole-2,4-dicarboxylate was then recrystallized from toluene and further reacted with formamidine acetate (0.207 mol) in ethanol (70 ml). The use of a smaller amount of ethanol [pyrrole–ethanol molar ratio = 1:24, compared with a molar ratio of 1:31 used by Kamath *et al.* (2009)] enabled direct isolation of methyl 4-oxo-4,5-dihydro-3*H*-pyrrolo[3,2-*d*]pyrimidine-7-carboxylate from the reaction solution. This intermediate was purified by recrystallization from acetic acid. The final reaction step was used without any modifications to achieve (I) as a beige solid. Colourless crystals suitable for X-ray studies were obtained by slow evaporation from a water solution.

IR (ν_{max}, cm^{-1}): 3265 (N—H)$_{ar}$, 3151, 3103, 3021 (C—H)$_{ar}$, 1663 (C=O), 1595, 1542, 1516, 1483 (C···C)$_{ring}$ and (C···N)$_{ring}$. ^{1}H NMR (DMF-d_7, TMS, 298 K): δ 12.15 (*bs*, 1H, HN^7), 11.82 (*bs*, 1H, HN^1), 7.93 (*s*, 1H, HC^2), 7.49 (*d*, J = 2.6 Hz, 1H, HC^8), 6.43 (*d*, J = 2.8 Hz, 1H, HC^9). ^{13}C NMR (DMF-d_7, TMS, 298 K): δ 154.1 (C6), 145.4 (C4), 141.9 (C2), 127.5 (C8), 118.6 (C5), 103.4 (C9). ^{15}N NMR (DMF-d_7, relative to DMF, 298 K): δ 140.42 [*d*, J = 101.2 Hz, 12.15, HN^7; *s*, 7.49, HC^8; *s*, 6.43, HC^9 (N7)], 166.6 [*s*, 47.93, HC^2 (N1)], 236.47 [*d*, J = 10.7 Hz, 7.93, HC^2 (N3)]. ESI+MS: m/z 136.1 [M + H]$^+$ (calculated = 136.1), 158.1 [M + Na]$^+$ (calculated = 158.1). Analysis calculated for $C_6H_5N_3O$: C 53.33, H 3.73, N 31.10%; found: C 53.46, H 3.70, N 31.44%.

Crystal data

$C_6H_5N_3O$
M_r = 135.13
Monoclinic, $P2_1/n$
a = 4.8315 (12) Å
b = 19.976 (5) Å
c = 6.3551 (13) Å
β = 104.69 (2)°
V = 593.3 (2) Å^3
Z = 4
Mo $K\alpha$ radiation
μ = 0.11 mm^{-1}
T = 100 K
0.20 × 0.15 × 0.10 mm

Data collection

Oxford Xcalibur diffractometer with a Sapphire2 detector (large Be window)
Absorption correction: multi-scan (*CrysAlis RED*; Oxford Diffraction, 2009)
T_{min} = 0.978, T_{max} = 0.989
3740 measured reflections
1050 independent reflections
693 reflections with $I > 2\sigma(I)$
R_{int} = 0.063

Refinement

$R[F^2 > 2\sigma(F^2)]$ = 0.049
$wR(F^2)$ = 0.102
S = 0.94
1050 reflections
91 parameters
H-atom parameters constrained
$\Delta\rho_{max}$ = 0.27 e Å^{-3}
$\Delta\rho_{min}$ = −0.17 e Å^{-3}

H atoms were located in difference maps and refined using a riding model, with C—H = 0.95 Å and N—H = 0.88 Å, and with U_{iso}(H) = 1.2U_{eq}(C,N).

Table 1
Comparison of selected bond angles (°) in (I), hypoxanthine and 9-deazainosine monohydrate.

Bond	(I)	Hypoxanthine, monoclinic	Hypoxanthine, triclinic†	9-Deazainosine monohydrate
C5—N7—C8	107.34 (18)	103.81 (11)	103.7 (1), 104.8 (1)	108.7 (2)
C8—N9/C9—C4	106.7 (2)	106.41 (11)	107.0 (1), 106.6 (1)	105.7 (2)
Reference	This work	(*a*)	(*b*)	(*c*)

† Two crystallographically independent molecules within the unit cell. References: (*a*) Yang & Xie (2007); (*b*) Schmalle *et al.* (1988); (*c*) Otter *et al.* (1992).

Table 2
Hydrogen-bond geometry (Å, °).

D—H···A	D—H	H···A	D···A	D—H···A
N1—H1···O1^{i}	0.88	1.92	2.799 (3)	175
N7—H7···N3^{ii}	0.88	2.09	2.965 (3)	176
C2—H2···O1^{iii}	0.95	2.18	3.106 (3)	165

Symmetry codes: (i) $-x+2, -y, -z+1$; (ii) $x, y, z+1$; (iii) $x, y, z-1$.

Data collection: *CrysAlis CCD* (Oxford Diffraction, 2009); cell refinement: *CrysAlis RED* (Oxford Diffraction, 2009); data reduction: *CrysAlis RED*; program(s) used to solve structure: *SHELXS97* (Sheldrick, 2008); program(s) used to refine structure: *SHELXL97* (Sheldrick, 2008); molecular graphics: *Mercury* (Macrae *et al.*, 2008) and *DIAMOND* (Brandenburg, 2011); software used to prepare material for publication: *publCIF* (Westrip, 2010) and *PARST* (Nardelli, 1995).

This work was supported financially by the Operational Program for Research and Development for Innovations of the European Regional Development Fund (grant No. CZ.1.05/2.1.00/03.0058), by the Operational Program for Education for Competitiveness of the European Social Fund (grant No. CZ.1.07/2.3.00/20.0017), by the Ministry of Education, Youth and Sports of the Czech Republic, and by Palacky University (grant No. PrF_2012_009). The authors thank Mrs Pavla Richterova for performing the CHN elemental analyses, Dr Igor Popa for the NMR spectroscopic measurements and interpretations, and Mr Dmytro Rak for assistance with the synthesis.

Supplementary data for this paper are available from the IUCr electronic archives (Reference: SK3467). Services for accessing these data are described at the back of the journal.

References

Allen, F. H. (2002). *Acta Cryst.* B**58**, 380–388.
Bantia, S., Miller, P. J., Parker, C. D., Ananth, S. L., Horn, L. L., Kilpatrick, T. L., Montgomery, J. A. & Sandhu, J. S. (2001). *Int. Immunopharmacol.* **1**, 1199–1210.
Bernstein, J., Davis, R. E., Shimoni, L. & Chang, N.-L. (1995). *Angew. Chem. Int. Ed. Engl.* **34**, 1555–1573.
Brandenburg, K. (2011). *DIAMOND*. Crystal Impact GbR, Bonn, Germany.
Bzowska, A., Kulikowska, E. & Shugar, D. (2000). *Pharmacol. Ther.* **88**, 349–425.
Čapek, P., Otmar, M., Masojídková, M., Votruba, I. & Holý, A. (2003). *Collect. Czech. Chem. Commun.* **68**, 779–791.
Clinch, K., Evans, G. B., Fröhlich, R. F., Furneaux, R. H., Kelly, P. M., Legentil, L., Murkin, A. S., Li, L., Schramm, V. L., Tyler, P. C. & Woolhouse, A. D. (2009). *J. Med. Chem.* **52**, 1126–1143.
Desiraju, G. R. & Steiner, T. (2001). In *The Weak Hydrogen Bond*. Oxford University Press.
Kamath, V. P., Juarez-Brambila, J. J., Morris, C. B., Winslow, C. D. Jr & Morris, P. E. (2009). *Org. Process Res. Dev.* **13**, 928–932.
Macrae, C. F., Bruno, I. J., Chisholm, J. A., Edgington, P. R., McCabe, P., Pidcock, E., Rodriguez-Monge, L., Taylor, R., van de Streek, J. & Wood, P. A. (2008). *J. Appl. Cryst.* **41**, 466–470.
Montgomery, J. A., Niwas, S., Rose, J. D., Secrist, J. A. III, Babu, Y. S., Bugg, C. E., Erion, M. D., Guida, W. C. & Ealick, S. E. (1993). *J. Med. Chem.* **36**, 55–69.
Nardelli, M. (1995). *J. Appl. Cryst.* **28**, 659.
Otmar, M., Masojídková, M., Votruba, I. & Holý, A. (2004). *Bioorg. Med. Chem.* **12**, 3187–3195.
Otter, B. A., Patil, S. A., Klein, R. S. & Ealick, S. E. (1992). *J. Am. Chem. Soc.* **114**, 668–671.
Oxford Diffraction (2009). *CrysAlis CCD* and *CrysAlis RED*. Oxford Diffraction Ltd, Yarnton, Oxfordshire, England.
Schmalle, H. W., Hänggi, G. & Dubler, E. (1988). *Acta Cryst.* C**44**, 732–736.
Sheldrick, G. M. (2008). *Acta Cryst.* A**64**, 112–122.
Sutton, J. M., *et al.* (2012). *Bioorg. Med. Chem. Lett.* **22**, 1464–1468.
Westrip, S. P. (2010). *J. Appl. Cryst.* **43**, 920–925.
Yang, R.-Q. & Xie, Y.-R. (2007). *Acta Cryst.* E**63**, o3309.

supplementary materials

Acta Cryst. (2013). C**69**, 158-161 [doi:10.1107/S0108270112050767]

Infinite ladder-like chains organized into a three-dimensional zigzag supramolecular architecture in 9-deazahypoxanthine

Radka Novotná and Zdeněk Trávníček

3*H*-pyrrolo[3,2-*d*]pyrimidin-4(5*H*)-one

Crystal data

$C_6H_5N_3O$
$M_r = 135.13$
Monoclinic, $P2_1/n$
Hall symbol: -P 2yn
$a = 4.8315$ (12) Å
$b = 19.976$ (5) Å
$c = 6.3551$ (13) Å
$\beta = 104.69$ (2)°
$V = 593.3$ (2) Å^3
$Z = 4$
$F(000) = 280$
$D_x = 1.513$ Mg m^{-3}
Mo $K\alpha$ radiation, $\lambda = 0.71073$ Å
Cell parameters from 1593 reflections
$\theta = 3.1$–$33.3°$
$\mu = 0.11$ mm^{-1}
$T = 100$ K
Prism, colourless
0.20 × 0.15 × 0.10 mm

Data collection

Oxford Xcalibur diffractometer with Sapphire2 detector (large Be window)
Radiation source: Enhance (Mo) X-ray Source
Graphite monochromator
Detector resolution: 8.3611 pixels mm^{-1}
ω scans
Absorption correction: multi-scan (*CrysAlis RED*; Oxford Diffraction, 2009)
$T_{min} = 0.978$, $T_{max} = 0.989$
3740 measured reflections
1050 independent reflections
693 reflections with $I > 2\sigma(I)$
$R_{int} = 0.063$
$\theta_{max} = 25.1°$, $\theta_{min} = 3.5°$
$h = -5 \rightarrow 5$
$k = -23 \rightarrow 22$
$l = -7 \rightarrow 7$

Refinement

Refinement on F^2
Least-squares matrix: full
$R[F^2 > 2\sigma(F^2)] = 0.049$
$wR(F^2) = 0.102$
$S = 0.94$
1050 reflections
91 parameters
0 restraints
Primary atom site location: structure-invariant direct methods
Secondary atom site location: difference Fourier map
Hydrogen site location: inferred from neighbouring sites
H-atom parameters constrained
$w = 1/[\sigma^2(F_o^2) + (0.0548P)^2]$ where $P = (F_o^2 + 2F_c^2)/3$
$(\Delta/\sigma)_{max} < 0.001$
$\Delta\rho_{max} = 0.27$ e Å^{-3}
$\Delta\rho_{min} = -0.17$ e Å^{-3}

Special details

Experimental. Elemental analysis (CHN) was performed on a Thermo Scientific Flash 2000 CHNO-S Analyzer. FT–IR spectra were recorded on a Thermo Nicolet Nexus 670 spectrometer equipped with a micro-ATR module (single reflection diamond ATR crystal) in the 400–4000 cm^{-1} range. The ^{1}H, ^{13}C and ^{15}N NMR spectra of the DMSO-d_6 or DMF-d_7 solutions were collected at 300 K on a Varian 400 spectrometer at 400.00, 100.58 and 40.53 MHz, respectively. ^{1}H and ^{13}C spectra were calibrated using tetramethylsilane as a reference. The ^{15}N NMR spectrum was measured relative to the DMF signals. Mass spectra (MS) were recorded on an LTQ Fleet (ThermoFisher Scientific) using the positive electrospray ionization (ESI+) and full scan mode in *ca* 10^{-5} *M* methanolic solutions.

Geometry. All e.s.d.'s (except the e.s.d. in the dihedral angle between two l.s. planes) are estimated using the full covariance matrix. The cell e.s.d.'s are taken into account individually in the estimation of e.s.d.'s in distances, angles and torsion angles; correlations between e.s.d.'s in cell parameters are only used when they are defined by crystal symmetry. An approximate (isotropic) treatment of cell e.s.d.'s is used for estimating e.s.d.'s involving l.s. planes.

Refinement. Refinement of F^2 against ALL reflections. The weighted *R*-factor *wR* and goodness of fit *S* are based on F^2, conventional *R*-factors *R* are based on *F*, with *F* set to zero for negative F^2. The threshold expression of $F^2 > \sigma(F^2)$ is used only for calculating *R*-factors(gt) *etc*. and is not relevant to the choice of reflections for refinement. *R*-factors based on F^2 are statistically about twice as large as those based on *F*, and *R*-factors based on ALL data will be even larger.

Fractional atomic coordinates and isotropic or equivalent isotropic displacement parameters ($Å^2$)

	x	*y*	*z*	U_{iso}*/U_{eq}
N1	0.7585 (4)	0.05060 (9)	0.2910 (3)	0.0185 (5)
H1	0.8929	0.0201	0.3028	0.022*
O1	0.7935 (3)	0.04177 (8)	0.6563 (2)	0.0220 (4)
C2	0.6453 (5)	0.07721 (12)	0.0909 (4)	0.0213 (6)
H2	0.7187	0.0616	−0.0254	0.026*
N3	0.4440 (4)	0.12250 (10)	0.0454 (3)	0.0215 (5)
C4	0.3504 (5)	0.14308 (11)	0.2234 (4)	0.0181 (6)
C5	0.4583 (5)	0.11720 (12)	0.4322 (4)	0.0173 (5)
C6	0.6780 (5)	0.06798 (11)	0.4763 (4)	0.0170 (5)
N7	0.3190 (4)	0.14745 (9)	0.5707 (3)	0.0193 (5)
H7	0.3475	0.1396	0.7108	0.023*
C8	0.1282 (5)	0.19201 (12)	0.4504 (4)	0.0209 (6)
H8	0.0036	0.2197	0.5063	0.025*
C9	0.1421 (5)	0.19112 (12)	0.2378 (4)	0.0212 (6)
H9	0.0327	0.2177	0.1224	0.025*

Atomic displacement parameters ($Å^2$)

	U^{11}	U^{22}	U^{33}	U^{12}	U^{13}	U^{23}
N1	0.0138 (10)	0.0211 (11)	0.0202 (11)	0.0040 (9)	0.0032 (8)	0.0018 (8)
O1	0.0185 (9)	0.0274 (10)	0.0198 (9)	0.0045 (7)	0.0045 (7)	0.0037 (7)
C2	0.0183 (13)	0.0257 (14)	0.0196 (13)	−0.0007 (12)	0.0040 (10)	−0.0015 (11)
N3	0.0168 (11)	0.0234 (12)	0.0237 (12)	0.0006 (9)	0.0039 (9)	0.0004 (9)
C4	0.0128 (12)	0.0188 (13)	0.0228 (14)	−0.0042 (10)	0.0046 (10)	−0.0013 (10)
C5	0.0135 (12)	0.0179 (13)	0.0209 (13)	−0.0034 (10)	0.0054 (10)	−0.0006 (10)
C6	0.0145 (12)	0.0173 (12)	0.0197 (13)	−0.0050 (10)	0.0052 (10)	−0.0014 (10)
N7	0.0161 (11)	0.0213 (11)	0.0202 (11)	0.0010 (9)	0.0042 (8)	0.0012 (8)
C8	0.0113 (11)	0.0176 (13)	0.0330 (15)	−0.0001 (10)	0.0045 (10)	−0.0004 (11)
C9	0.0122 (12)	0.0207 (14)	0.0278 (15)	0.0013 (10)	−0.0001 (10)	0.0037 (11)

Geometric parameters (Å, º)

N1—C2	1.358 (3)	C4—C9	1.410 (3)
N1—C6	1.375 (3)	C5—N7	1.376 (3)
N1—H1	0.8800	C5—C6	1.422 (3)
O1—C6	1.253 (3)	N7—C8	1.367 (3)
C2—N3	1.306 (3)	N7—H7	0.8800
C2—H2	0.9500	C8—C9	1.370 (3)
N3—C4	1.383 (3)	C8—H8	0.9500
C4—C5	1.396 (3)	C9—H9	0.9500
C2—N1—C6	124.7 (2)	O1—C6—N1	121.3 (2)
C2—N1—H1	117.7	O1—C6—C5	127.3 (2)
C6—N1—H1	117.7	N1—C6—C5	111.4 (2)
N3—C2—N1	125.4 (2)	C8—N7—C5	107.34 (18)
N3—C2—H2	117.3	C8—N7—H7	126.3
N1—C2—H2	117.3	C5—N7—H7	126.3
C2—N3—C4	113.9 (2)	N7—C8—C9	110.4 (2)
N3—C4—C5	123.1 (2)	N7—C8—H8	124.8
N3—C4—C9	130.0 (2)	C9—C8—H8	124.8
C5—C4—C9	106.9 (2)	C8—C9—C4	106.7 (2)
N7—C5—C4	108.7 (2)	C8—C9—H9	126.7
N7—C5—C6	129.8 (2)	C4—C9—H9	126.7
C4—C5—C6	121.6 (2)		

Hydrogen-bond geometry (Å, º)

D—H···*A*	*D*—H	H···*A*	*D*···*A*	*D*—H···*A*
N1—H1···O1^{i}	0.88	1.92	2.799 (3)	175
N7—H7···N3^{ii}	0.88	2.09	2.965 (3)	176
C2—H2···O1^{iii}	0.95	2.18	3.106 (3)	165

Symmetry codes: (i) −*x*+2, −*y*, −*z*+1; (ii) *x*, *y*, *z*+1; (iii) *x*, *y*, *z*−1.

Comparison of selected bond angles (°) in (I), hypoxanthine and 9-deazainosine monohydrate

Bond	(I)	Hypoxanthine, monoclinic	Hypoxanthine, triclinic*	9-Deazainosine monohydrate
C5—N7—C8	107.34 (18)	103.81 (11)	103.7 (1), 104.8 (1)	108.7 (2)
C8—N9/C9—C4	106.7 (2)	106.41 (11)	107.0 (1), 106.6 (1)	105.7 (2)
Reference	This work	(a)	(b)	(c)

Note: (*) two crystallographically independent molecules within the unit cell. References: (a) Yang & Xie (2007); (b) Schmalle *et al.* (1988); (c) Otter *et al.* (1992).